Thermal Rectification in Liquids by Manipulating the Solid-Liquid Interface

Sohail Murad[*†] *and Ishwar K. Puri*

[*]Department of Chemical Engineering, University of Illinois at Chicago, Chicago, Illinois 60607, USA and [†]Department of Engineering Science and Mechanics, Virginia Tech, Blacksburg, Virginia 24061, USA

Abstract

Thermal rectification, the origin of which lies in modifying the thermal resistance in a nonlinear manner, could significantly improve the thermal management of a wide range of nano-devices (both electronic and thermoelectric), thereby improving their efficiencies. Since rectification requires a material to be inhomogeneous, it has been typically associated with solids. However, the structure of solids is relatively difficult to manipulate, which makes the tuning of thermal rectification devices challenging. Since liquids are more amenable to tuning, this could open up new applications for thermal rectification. We use molecular dynamics simulations to demonstrate thermal rectification using liquid water. This is accomplished by creating an inhomogeneous water phase, either by changing the morphology of the surface in contact with the liquid or by imposing an arbitrary external force, which in practice could be through an electric or magnetic field. Our system consists of a bulk fluid that is confined in a reservoir that is bounded by two walls, one hot and the other cold. The interfacial (Kapitza) thermal resistance

[†] Author for correspondence -- murad@uic.edu

at the solid-fluid interface and the density gradient of the bulk fluid both influence the magnitude of the thermal rectification. However, we find that the role of the interfacial resistance is more prominent than the application of an external force on the bulk fluid. This observation presents opportunities to develop different types of switches for changing the direction of thermal rectification by manipulating surface morphology or externally driven molecular forces.

Mass disorder in a nanomaterial modifies its thermal conductivity k.[1, 2] An organized anisotropic structure leads to a systematically varying gradient for k.[3] Studies a structured molecular organization produced by mixing two materials,[4] by applying a uniform local force to displace their molecules in a preferred direction,[3] or through topological asymmetry,[5] there is greater heat flow in the direction of decreasing mass density, but a smaller such flux in the opposite direction.[5] For such cases, k, and the heat flux q'', both depend upon the direction in of the imposed temperature gradient ($\Delta T/\Delta x$). This directional variation of q'' forms the basis for thermal rectification, $q''_{L\to R} \neq q''_{R\to L}$, where L and R denote its left and right faces. Mathematically, a sufficient condition for rectification is that the position and temperature dependence in thermal conductivity, is not functionally separable, i.e.,

$$k(x,T) \neq f(x)\, g(T). \qquad (1)$$

For homogeneous materials, Eq. (1) cannot be satisfied as k only depends upon temperature. It has therefore been generally assumed for rectification one must have layered composite materials.[6, 7]

The more interesting applications of rectification are expected to be at the nanoscale,[4, 6, 7] e.g., in nanodevices for the thermal management. Rectification allows material behavor both as a conductor and an insulator. Thus, it could also contribute to improving sustainability solutions, such as solar water heaters.[8] Other possible applications include biomedical devices, thermal computers, etc.[9]

Thermal rectification has been observed using molecular dynamics (MD) in solids such as graphene,[4] and argon/krypton interfaces.[10] Solids have fixed structures that cannot be modified readily. Hence, while tunability is possible, e.g., by applying mechanical stress, a recent study[11] of zigzag graphene nanoribbons only weak thermal conductivity dependence at typical tensile strains. Hence, structural manipulations to obtain thermal rectification can be expected to be

typically much more energy intensive in solids than in liquids. If liquids were to be used in thermal rectification devices, then their structures could be more easily manipulated. This would greatly facilitate tuning.

Intersecting materials create interfaces and k and q'' depend upon the interfacial (Kaptiza) thermal resistance R_k.[12-16] R_k depends on the hydrophobic or hydrophilic nature of the interfaces in a solid-fluid system.[13, 14, 16] The influence of the interfacial resistance is schematically discussed in Fig. 1 for a typical system with interfaces. If both walls are hydrophobic (Case 1), two interfacial resistances of $O(\delta_t)$ are observed. This leads to a bulk resistance $R_b = (L\text{-}\delta_t)/k_m$ in the reservoir, where k_m denotes the bulk fluid conductivity, and interfacial resistances $R_{f,c}$ and $R_{f,h}$ in the cold and hot fluid boundary layers.[13, 14, 17] If fluid molecules are uniformly displaced by a small force towards the cold wall (cade 2), the interfacial layer width on the cold side decreases, and consequently, so does $R_{f,c}$.[3] However, here, $R_{f,h}$ increases since the fluid is now further displaced from the hot wall. This counterbalancing effect is very significant. Making the cold wall hydrophilic in Case 3 enables the adsorption of water molecules on its surface, further decreasing $R_{f,c}$ through this nanoscale effect.

The influence of interfacial solid-fluid interactions on thermal rectification is yet unclear.[3] However, since the resistances shown in Fig. 1 lie in series, decreasing any one should diminish the overall resistance to heat transfer and enhance q''. We hypothesize that, because R_k decreases with increasing temperature,[13, 17] $R_{f,c}$ should be manipulated to obtain greater rectification in a solid-fluid system rather than the interfacial resistance $R_{f,h}$, or R_b. We investigate this hypothesis using MD simulations, which also allow us to discriminate between localized nanoscale interfacial effects and bulk consequences.

The simulations consider thermal transport across hot and cold solid-fluid interfaces that enclose a bulk fluid in two adjacent reservoirs of equal volume. The walls influence small portions of the fluid adjacent to them, but the remaining fluid in the reservoirs exhibits bulk properties [3,13, 14, 17] with the water density ρ=487.5 kg/m^3. The system consists of 1024 molecules each of water and silicon, as shown in Fig. 2. The two walls, one hot and the other cold, consist of 512 Si atoms each. Test runs were done with a system twice this size and the results did not change qualitatively. All Si atoms are tethered to their equilibrium sites and allowed to vibrate harmonically. The molecules in the system are provided with initial Gaussian velocity distributions and the silicon walls are imparted average hot and cold temperatures T_h = 1209 K and T_c = 403 K with a Gaussian thermostat. This arrangement results in an average fluid temperature T_m = (T_h+T_c)/2 = 806 K that is relatively invariant to the heat flux across the reservoirs. At this average temperature, the bulk fluid is supercritical. These relatively high wall temperatures facilitate larger heat transfer rates and minimize data scatter. However, the fundamental aspects of rectification remain unaltered and apply even at lower temperatures.[3] The (N,V,T) simulations proceed with uniform step sizes of 1 fs, and are allowed to equilibrate. Results are reported when simulations that have progressed by 2×10^6 time steps and reached a steady state. Longer simulations have confirmed the accuracy and stability of the temperature and density profiles.[3]

The MD algorithm uses the quaternion method.[18] Intermolecular interactions follow the potential model $u_{ij} = 4\varepsilon_{ij}((\sigma_{ij}/r_{ij})^{12} - (\sigma_{ij}/r_{ij})^{6}) + (q_i q_j)/r_{ij}$, where σ_{ij} and ε_{ij} denote the L-J interaction parameters, r_{ij} the scalar distance between sites i and j, and q_i and q_j the charges on these sites. The SPC potential is used for water, which represents water properties realistically[19] (including thermal conductivity [20]) Si is modeled with an L-J potential while three-body

interactions are indirectly enforced for the coordinated tetrahedral bonded structure of Si by tethering these atoms to their equilibrium sites.[21] Cross interactions are modeled using Lorentz-Berthelot mixing rules and the reaction field method [22] replicates long-range interactions. [23, 24] A cutoff distance of 9.5Å is used. The wall width is 2.05 nm so it screens the molecules on one side from the other.

To investigate bulk effects, we apply a small external force of 0.732 pN in the x-direction to each water molecule, creating a density gradient in the bulk fluid towards the cold wall for Case 2 and the hot wall for Case 2a. The intermolecular forces in water are larger than this applied force by at least an order of magnitude. The forces on the fluid molecules in the central section, which lies between the two Si walls, are applied in an opposite direction to those imposed on water molecules on either side of these two enclosing walls. The interaction between water and the Si surface is hydrophobic, since it primarily involves noncoulombic van der Waals (LJ only in our simulations) interactions. The Si surface is then prepared to mimic a hydrophilic interface by manipulating q_i and q_j. The values of the charges on adjacent atoms are specified as positive and negative ($+q$, $-q$) to mimic a polar surface. The cold wall is made hydrophilic in Case 3 and the hot wall for Case 3a. The system is divided in the x-direction into 138 slabs of 0.146 nm lengths and 6.09×10^{-28} m^3 volumes within which the local properties are averaged.

Figure 3(a) presents the bulk water density in the hot and cold reservoirs and temperature profiles for Cases 1-3, i.e., when (1) both enclosing walls of the reservoirs are hydrophobic with no forces, (2) all fluid molecules are uniformly subjected to a force F = 0.732 pN towards the cold wall that produces a bulk effect and alter R_b, and (3) both faces of the cold wall are made hydrophilic by the inclusion of alternating charges of 0.75 e^- to investigate the localized nanoscale interfacial effect on $R_{f,c}$. The number of water molecules N averaged in each of the 138

sections represents the local density. In the absence of an applied force or hydrophilic solid-fluid interactions at the interfaces, the fluid density on the colder side of the reservoir is larger than the warmer side, which is to be expected. N increases slightly adjacent to the cold wall when an external force is applied as compared to the case for a hydrophobic wall.[3] Overall, since the two values of N on the cold side are of similar magnitude, the corresponding interfacial resistance is also comparable for Cases 1 and 2 as exhibited through the temperature profiles for these two cases, which are alike. Consequently, the corresponding heat fluxes are not too dissimilar. There is a greater increase in the fluid density for Case 3 when the cold wall is hydrophilic due to the nanoscale adsorption and layering of fluid molecules[13, 14, 17, 25, 26] as compared to Cases 1 and 2. This effect significantly decreases the interfacial resistance to heat transfer[17, 25] so that the temperature profile for Case 3 exhibits a steeper bulk temperature gradient than the other two cases do, thereby leading to a larger overall heat flux. Essentially, the results show that altering $R_{f,c}$ has a more significant influence than changing R_b by the external force that is applied.

The corresponding hot wall results, i.e., when a constant force oriented towards the hot wall is applied to all water molecules (Case 2a), or both faces of the hot walls are made hydrophilic (Case 3a) are presented in Fig. 3(b). Case 1, with hydrophobic walls and no external force imparted is also included in the figure for comparison. Again, the applied force is less effective than are the hydrophilic water-Si interactions. Hence, when the hot walls are rendered hydrophilic for Case 3a, the corresponding heat flux exceeds that for Cases 1 and 2a. This again shows that nanoscale interfacial effects that modify $R_{f,h}$ are more effective at modifying the thermal transport than when the fluid bulk is rearranged through the imposition of an external force field and R_b is altered. Our simulations also show that when only an external force is used,

reorienting the water molecules with an external electric field does not change the temperature profiles measurably.

Increasing the values of the (+q, -q) charges makes a wall more hydrophilic. Hence, in Fig. 4, the magnitude of the charge imparted to the (i,j) sites is a measure of the wall's hydrophilic nature. The figure shows that the heat flux increases with increasing *charge*, i.e., making either of the hot or cold walls more hydrophilic also enhances the overall thermal transport through the reservoir. However, consistent with our hypothesis, making the cold wall hydrophilic and diminishing $R_{f,c}$ allows for greater heat transfer than is possible with a similar hydrophilic hot wall by decreasing $R_{f,h}$.

The slopes of heat flux *vs.* e^- for the two conditions illustrate this response. The hydrophilic cold wall that includes Case 3 is greater than the corresponding hot wall set that includes Case 3a by 75%. Making the cold wall increasingly hydrophilic by increasing the electron charge imparted to (i,j) sites, thus adsorbing more fluid molecules on it, increases q'' substantially more than when these charges are imparted to the hot wall. This observation forms the basis for thermal rectification $r_{\alpha-1} = (q''_\alpha - q''_1)/q''_1$, where q''_1 denotes the heat flux for Case 1 and q''_α the flux when the bulk fluid is displaced towards the cold or hot walls, or the hydrophobic walls are modified to become more hydrophilic. Clearly, in the reservoir, when the hydrophilic wall is on the cold side, q''_α is larger than when this wall is placed on the hot side. Thermal rectification devices that include fluid-solid interfaces should therefore focus on reducing the interfacial resistance on the cold side as rectification is more sensitive to the hydrophilicity of the cold wall.

The surface modification results presented here are in contrast to those obtained when the bulk density and, hence, R_b are manipulated. As shown in Fig. 4, in comparison with Case 1 (with 0 e^-, 0 pN), displacing the fluid molecules towards the cold wall through a bulk effect by decreasing

the value of $-F$ diminishes the heat flux, i.e. $r_{\alpha-1}$ is $-ve$. Moving the fluid closer to the hot wall (with $+F$) increases $r_{\alpha-1}$.[3] This is consistent with previous results that also show a greater heat flow in the direction of decreasing mass density in a nanomaterial.[4] Imparting an external force to each fluid molecule results in a similar density grading, producing an asymmetric bulk thermal conductance. Hence, increasing the fluid density adjacent to a hot wall, e.g., by moving the entire fluid closer towards it through an external force, as for Case 2a, enhances the bulk thermal conductivity, but moving it towards the cold wall has the opposite effect of lowering the bulk conductivity, which reduces thermal transport.

The set that includes Case 2a, for which q''_α and $r_{\alpha-1}$ decrease with increasing $|F|$, thus behaves unlike the three sets that include Cases 2, 3 and 3a. Denoting these sets as II (which contains Case 2), IIa (with Case 2a), III (containing Case 3) and IIIa (with Case 3a), we summarize that $r_{III-1} > r_{IIIa-1}$ and $r_{IIa-1} > r_{II-1}$. While $r_{II-1} < 0$, the other three cases allow for positive values of the thermal rectification.

Consequently, the direction of thermal rectification for the sets II and IIa that include Cases 2 and 2a is different from that for sets III and IIIa that include Cases 3 and 3a. This suggests opportunities to develop switches to change the direction of thermal rectification by focusing either on surface modifications or bulk density gradients, or appropriate combinations of the two, e.g., by using external force fields such electric or magnetic fields. In addition, when rectification results from rendering a surface hydrophilic, it has a more significant influence on the magnitude of thermal transport than when an external force is applied to the bulk fluid.

In summary, we show that by either using an external force or by modifying the solid surface in contact with a fluid, we can demonstrate thermal rectification in liquids. Liquid based rectification devices will be more easily amenable to tuning. An external force constitutes a bulk

effect, while modifying either of the walls to make them hydrophilic, results in a localized nanoscale interfacial influence. In either case, the direction in which effect is implemented changes the overall value of k so that $q''_{L\to R} \neq q''_{R\to L}$. The origin of the thermal rectification $r_{\alpha\text{-}1}$ lies in modifying the thermal resistance in a nonlinear manner, e.g., by making the resistance arrangement asymmetric. The simulations confirm our hypothesis that, because R_k decreases with increasing temperature, manipulating the cold side resistance provides greater opportunities for rectification in a solid-fluid system rather than when the hot-side resistance is varied. In contrast, the overall thermal conductivity and, therefore, heat transfer are enhanced when the bulk fluid is displaced towards the hot wall. As a result, the direction of thermal rectification for surface modification effects is different from when the bulk fluid is displaced. This suggests opportunities to develop switches that enable changes in the direction of thermal rectification in devices.

This research was supported in part by grants from the National Science Foundation (CBET 1246536)

1. G. Balasubramanian, I. K. Puri, M. C. Bohm and F. Leroy, Nanoscale **3** (9), 3714-3720 (2011).
2. S. Pal, G. Balasubramanian and I. K. Puri, The Journal of Chemical Physics **136** (4), 044901-044907 (2012).
3. S. Murad and I. K. Puri, Applied Physics Letters **100** (12), 121901-121905 (2012).
4. C. W. Chang, D. Okawa, A. Majumdar and A. Zettl, Science **314** (5802), 1121-1124 (2006).
5. J. Hu, X. Ruan and Y. P. Chen, Nano Lett **9** (7), 2730-2735 (2009).

6. M. Peyrard, EPL (Europhysics Letters) **76**, 49 (2006).

7. C. Dames, Journal of Heat Transfer **131**, 061301 (2009).

8. B. Norton and S. Probert, Applied Energy **14** (3), 211-225 (1983).

9. N. Boechler, G. Theocharis and C. Daraio, Nature Materials **10** (9), 665-668 (2011).

10. N. Roberts and D. Walker, Journal of Heat Transfer **133**, 092401 (2011).

11. K. Gunawardana, K. Mullen, J. Hu, Y. P. Chen and X. Ruan, Arxiv preprint arXiv:1011.3033 (2010).

12. P. L. Kapitza, Journal of Physics, USSR **4**, 181 (1941).

13. S. Murad and I. K. Puri, Applied Physics Letters **92** (13), 133105 (2008).

14. S. Murad and I. K. Puri, Chemical Physics Letters **476** (4-6), 267-270 (2009).

15. G. L. Pollack, Reviews of Modern Physics **41** (1), 48-81 (1969).

16. P. A. E. Schoen, B. Michel, A. Curioni and D. Poulikakos, Chemical Physics Letters **476** (4-6), 271-276 (2009).

17. S. Murad and I. K. Puri, Chemical Physics Letters **467** (1-3), 110-113 (2008).

18. D. J. Evans and S. Murad, Molecular Physics **34** (2), 327-331 (1977).

19. J. Chandrasekhar, S. F. Smith and W. L. Jorgensen, Journal of the American Chemical Society **106** (10), 3049-3050 (1984).

20. W. Evans, J. Fish, and P. Keblinski, Journal of Chemical Physics, 126, 154504 (2007).

21. S. Murad and I. K. Puri, Applied Physics Letters **95** (5), 051907 (2009).

22. R. Gargallo, P. H. Hunenberger, F. X. Aviles and B. Oliva, Protein Science **12** (10), 2161-2172 (2003).

23. I. G. Tironi, R. Sperb, P. E. Smith and W. F. Vangunsteren, Journal of Chemical Physics **102** (13), 5451-5459 (1995).

24. H. J. C. Berendson, J. Postma and W. F. van Gunsteren, in *Intermolecular Forces*, edited by B. Pullman (Reidel, Dordecht, 1981).

25. G. Balasubramanian, S. Banerjee and I. K. Puri, Journal of Applied Physics **104** (6), 064306 (2008).

26. S. Murad and I. K. Puri, Physics of Fluids **19**, 128102 (2007).

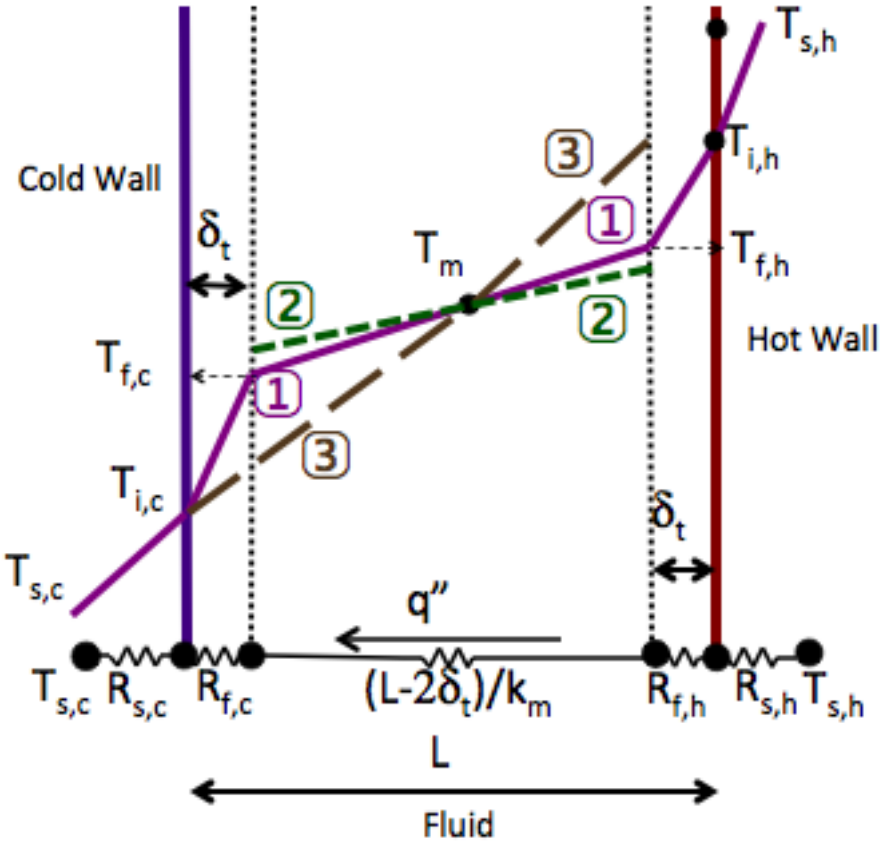

Figure 1. Schematic diagram of the thermal resistance across the hot and cold fluid–solid interfaces. A reservoir at a mean temperature T_m is contained within two solid walls of thickness L. The δ_t thick thermal boundary layers adjacent to the walls are bounded by the fluid temperatures $T_{f,c}$ and $T_{f,h}$, and interface temperatures $T_{i,c}$ and $T_{o,h}$ on the cold (c) and hot (h) sides, respectively. The thermal resistances $R_{f,h}$ and $R_{f,c}$ on the hot and cold fluid interfaces respectively produce the temperature discontinuities $\Delta T_h = T_{f,c}\text{-}T_{i,c}$ and $\Delta T_c = T_{f,h}\text{-}T_{i,h}$. The bulk fluid resistance $R_b = (L - \delta_t)/k_m$, where k_m denotes the mean bulk fluid thermal conductivity. The temperature profiles are labeled for Cases 1, 2 and 3 discussed in the text.

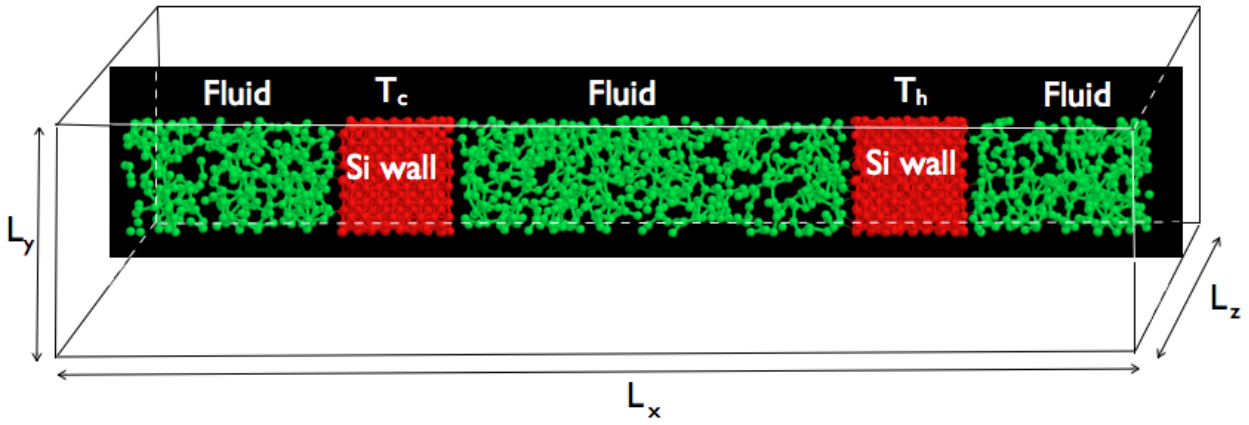

Figure 2. Schematic of the simulation domain, where L_x =20.2, and L_y = L_z =2.04 nm. The system is divided into 138 slabs of 0.146 nm lengths along L_x, each with a volume of 6.09×10^{-28} m^3. The Si walls include slabs 30-43 and 99-113.

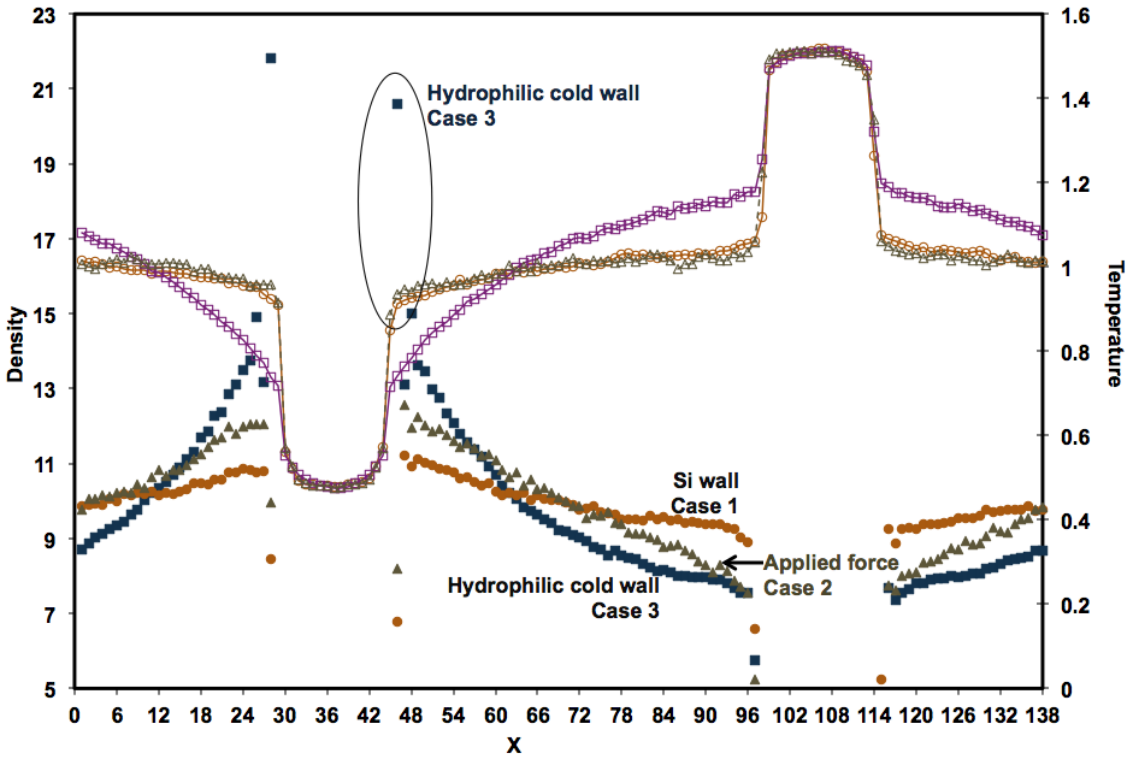
Hydrophilic cold wall
Case 3
Si wall
Case 1
Applied force
Case 2
Hydrophilic cold wall
Case 3
Density
Temperature
X

(a)

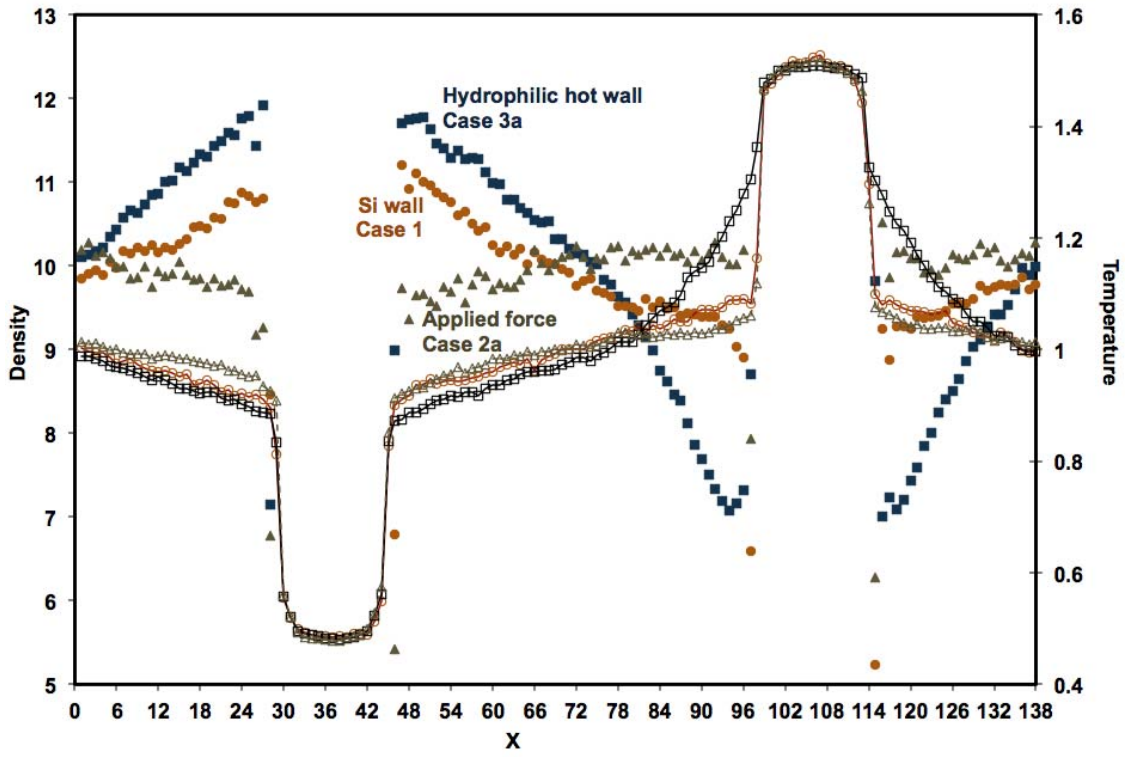
Hydrophilic hot wall
Case 3a
Si wall
Case 1
Applied force
Case 2a
Density
Temperature
X

(b)

Figure 3. The water density (closed symbols) in the hot and cold reservoirs, and the temperature profiles (open symbols) for the three cases a a function of the position numbers of the 138 slabs. The number of water molecules N averaged in each of the sections is taken as a surrogate for the local density. The dimensionless temperatures for a slab should be multiplied by 806 K to recover the units of K. (a) For Case 1 (●,○), both enclosing walls of the reservoirs are hydrophobic, for Case 2 (▲,△) all fluid molecules are uniformly displaced by a force F = 0.732 pN towards the cold wall, and for Case 3 (■,□) both faces of the cold wall are made hydrophilic by the inclusion of alternating charges of 0.75 e^-. (b) Case 1 (●,○),Case 2 (▲,△) when all fluid molecules are uniformly displaced by a force F = 0.732 pN towards the hot wall, and Case 3 (■,□) when both faces of the hots wall are made hydrophilic by the inclusion of alternating charges of 0.75 e^-.

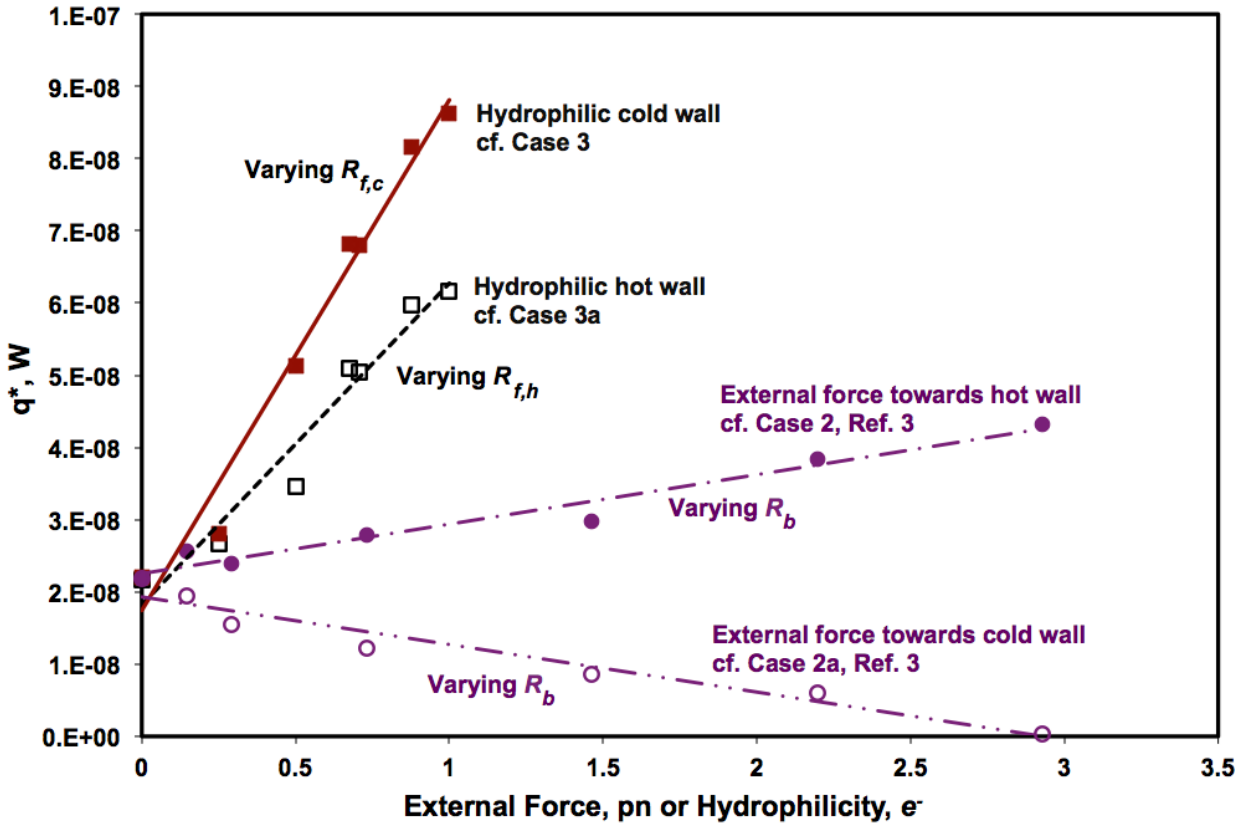

Figure 4. The variation in the heat flux in units of W with the magnitude of the hydrophilic nature of a hot (■) or cold (□) wall, and with the imposition of an external force on each fluid molecule[3] (●). The magnitude of the electron charge imparted to the (*i,j*) sites in units of e^- is taken as a surrogate for a wall's hydrophilic nature. For reference, the charge on a monovalent ion such as Cl^- is $1e^-$. The slope of the heat flux for increasing charge on the cold wall is 75% greater than the corresponding slope for a cold wall. In comparison with Case 1 (with 0 e^-, 0 pN), displacing the fluid molecules towards the cold wall through a bulk effect by decreasing $-F$ diminishes the heat flux. However, making the cold wall increasingly hydrophilic by increasing the electron charge imparted to (*i,j*) sites, thus adsorbing more fluid molecules on it, substantially increases q''.